effects between naked ANT and the s-SPG/ANT complex using the Promega *E. coli* T7 S30 system.

In the next step, we examined the antisense effect when intentionally added Exonuclease I (0.2 or 0.5 units/ml) to the system. This examination needed a completely nuclease-free (or nuclease-inhibited) T7 S30 extracted solution. For this purpose, we used Novagen's *E. coli* T7 S30 extract solution. According to their technical note [15] (EcoPro™ System), "The EcoPro System will function with a variety of DNA templates containing T7 or *E. coli* promoters upstream from coding sequence, including super-coiled, liner DNA and PCR products." Therefore, Novagen's *E. coli* T7 S30 extract solution can be considered practically nuclease-free. In fact, our data (Fig. 4) confirm that there is no detectable amount of active nuclease left in the extract solution.

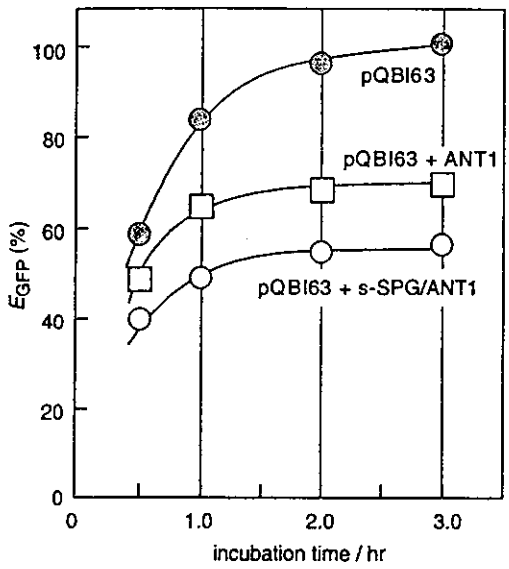

Fig. 1. Anti-sense affects on GFP expression efficiency (E_{GFP}) during incubation at 37°C in the *E. coli* T7 S30 extract system (Promega). pQBI template DNA system (control), filled circles; pQBI + ANT1, unfilled squares; pGBI + ANT1/s-SPG, unfilled circles. 1 μg of pQBI 63 was added to 50 μl of *E. coli* extract solution and incubated. E_{GFP} is defined by dividing the measured fluorescence intensity by that of the control (incubated for 3 h).

3. Results and discussion

3.1. Antisense effect and incubation time

To determine the optimal incubation time to compare antisense effects, the following three typical systems: pQBI63 itself (control), a mixture of pQBI63 and ANT1 (naked AN ODN), and a mixture of pQBI63 and s-SPG/ANT1 (complex) were examined. We added each of them to Promega's *E. coli* T7 S30 extract solution and measured GFP expression efficiency (E_{GFP}) against incubation time. The results are presented in Fig. 1. Here, E_{GFP} is defined by dividing the measured fluorescence intensity of each assay by that of the control incubated for 3 h. As shown in the figure, GFP expression seems saturated after 2–3 h. When three combinations are compared after 3 h, E_{GFP} for the naked ANT1 (in the figure denoted by pQBI63 + ANT1) is reduced to 70% of the control, and to 50% of the control for the pQBI63 + s-SPG/ANT1 complex. Although the data are not plotted, a mixture of pQBI63 and s-SPG (without ANT) shows almost the same features as the control, indicating that the presence of s-SPG in the system provides no influence on GFP expression (see below for details).

In the *E. coli* T7 S30 extract solution, sufficient amounts of NTP (nucleoside triphosphates), essential amino acids as well as other necessary components for protein expression exist [12]. Furthermore, AN ODNs should not consume those components or inhibit their functions, except through the GFP expression. Therefore, the saturated values of E_{GFP} in Fig. 1 should reflect the total amount of the mRNA translated to GFP. Thus, lower E_{GFP} values for pQBI63 + s-SPG/ANT1 and pQBI63 + ANT1 over controls can be explained by antisense effects [13,14]. Furthermore, differences between pQBI63 + ANT1 and pQBI63 + s-SPG/ANT1 should be related to the presence of the complex. After incubation for 3 h, E_{GFP} seems saturated for all three systems. Therefore, hereinafter, only E_{GFP} after incubation for 3 h was compared.

3.2. Comparison of the GFP expression efficiency using carriers and ANTs

Fig. 2 summarizes GFP expression efficiencies (E_{GFP}) (incubation time is 3 h for all measurements; E_{GFP} is defined by dividing the measured fluorescence intensity by that of the control). The control is indicated as the filled bar [pQBI63, Control (1)] in the histogram of Fig. 2. To examine whether polysaccharides interfere with the assay system, we added 50 μg of each polysaccharide (dextran, amylose, triple helix of schizophyllan or single chain of schizophyllan) to the standard: Fig. 2 assays (2)–(5). By comparing them, it is clear that simple presence of those polysaccharides does not provide any interference to normal GFP expression. When we added each ANT sample to the standard (ANT1;(6), ANT2;(7) and ANT3 (8)), values for E_{GFP} are reduced to about 75% of the control. This reduction should be ascribed to antisense effects. There is no significant difference among the three ANT samples, showing that the antisense effect is nearly the same for all three samples. The assays from (9) to (16) present the $M_{s\text{-}SPG}/M_{ANT}$ dependence of E_{GFP} for the ANT1 + s-SPG system. This series of assays shows that

E_{GFP} decreases with increasing the s-SPG molar ratio, and reaches a minimum at $M_{s\text{-}SPG}/M_{ANT} = 1.0$, then increases. When $M_{s\text{-}SPG}/M_{ANT} \geq 4$, the assay solution was opaque due to precipitation. Poor solubility or precipitation was sometimes observed when the assay mixture contained excess s-SPG to polynucleotides. The increment in E_{GFP} in the assays (14)–(16) in Fig. 2 can be ascribed to presence of the insoluble component of the complex. Since the lowest E_{GFP} is attained at $M_{s\text{-}SPG}/M_{ANT} = 1$, all measurements were carried out at this composition (including the preliminary examination in Fig. 1).

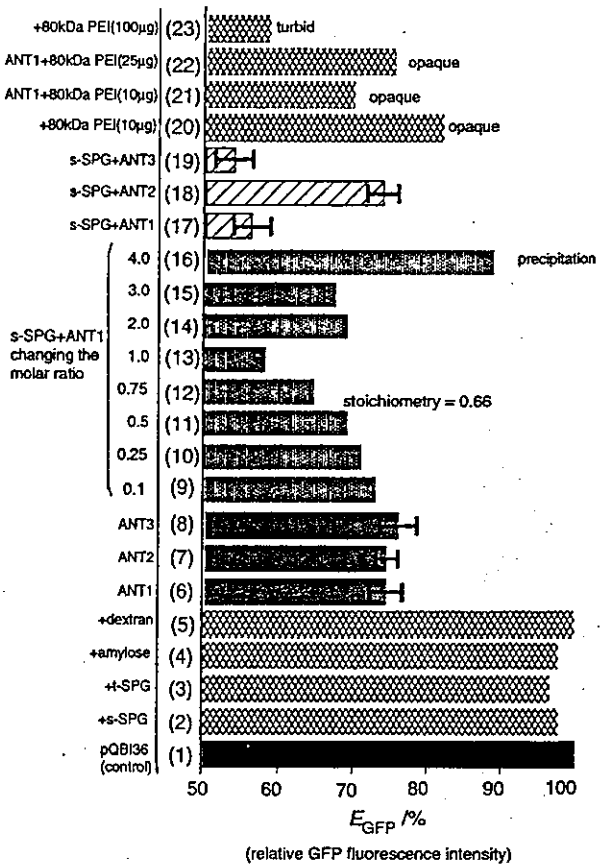

Fig. 2. Comparison of GFP expression efficiency (E_{GFP}) after incubation for 3 h, assay (1): pQBI template DNA only (control), 1 μg of pQBI 63 added to 50 μl of *E. coli* extract solution. Assays (2)–(5): each polysaccharide (100 μg) was added to the reference, t-SPG and s-SPG refer to triple helix and single chains of schizophyllan, respectively. Assays (6)–(8): 10 μg of each ANT was added to the standard. Assays (9)–(16): the mixture of s-SPG and ANT1 (complexes formed) were added to the standard numbers on the left-hand side show the $M_{s\text{-}SPG}/M_{ANT}$ molar ratio. Assays (17)–(19): comparison of ANT1+s-SPG (complex), ANT2+s-SPG (no complex), and ANT3+s-SPG (complex). (20): 10 μg of 80 kDa PEI (polyethyleneimine) was added to the standard. Assay (21): 10 μg of ANT1 was mixed with 10 μg of 80 kDa PEI and the mixture was added to the standard. Assay (22): 10 μg of ANT1 was mixed with 25 μg of 80 kDa PEI and the mixture was added to the standard. Assay (23): 100 μg of 80 kDa PEI was added to the standard.

As already shown [8], ANT2 cannot bind the s-SPG due to the short poly(dA) tail. This fact can then explain why there is no difference in E_{GFP} between naked ANT2 (assay (7)) and the mixture of ANT2 and s-SPG (assay (18)). On the other hand, ANT1 and ANT3 do form complexes with s-SPG. When ANT1 and ANT3 are added as the complex (assays (17) and (19)), E_{GFP} is drastically reduced. To confirm whether these differences in E_{GFP} between naked ANTs and complexed ANTs are statistically different from each other, we calculated the dispersion and t-value (Table 2). The results clarifies that the averaged E_{GFP} between naked ANTs and complexed ANTs are statistically different. The Promega *E. coli* T7 S30 extract solution is well-known to contain some amount of nuclease. Thus, protein expression from liner DNAs is significantly reduced because of DNA hydrolysis [18]. Therefore, when ANTs are added to this system, they should also suffer hydrolysis from intrinsic nuclease activity. Our previous paper revealed that nuclease-mediated hydrolysis of polynucleotides is drastically reduced in the complex [8]. Furthermore, we have directly proven that both s-SPG/ANT1 and s-SPG/ANT3 complexes show a lower hydrolysis rate than the corresponding naked ANTs [8]. Considering these two facts (presence of nuclease in the system, and low hydrolysis of complexed nucleotides), the low E_{GFP} for the complex can be explained by s-SPG protection of bound ANT and increased amount of ANT to bind mRNA, resulting to prohibit GFP expression.

PEI is used as an AS ODN positive control carrier, with 10 μg of PEI to 1 μg of pQBI63, and determination of E_{GFP}. As shown in Fig. 2, assay (20), E_{GFP} is reduced to 80%. It should be pointed out that even though no ANT is present, E_{GFP} is decreased in this PEI case. We also found that the solution becomes slightly opaque when PEI is added to the pQBI63 solution. This is probably due to complexation between cationic PEI and anionic pQBI63. Therefore, the observed reduced E_{GFP}

Table 2
Statistical analysis of the antisense test for the assays (6)–(7) and (17)–(19) in Fig. 2

	ANT1	ANT1+s-SPG	ANT2	ANT2+s-SPG	ANT3	ANT3+s-SPG
Average	56.4	74.5	74.0	75.3	54.0	75.3
Dispersion	4.3	4.3	2.5	2.9	6.5	4.3
n	5	4	5	4	5	4
t-value	15.1		3.9		15.4	

can be ascribed to the reduced plasmid. This interaction becomes more prominent when 100 μg of PEI are added to 1 μg of pQBI63, thus E_{GFP} in assay (23) is lower than that of assay (20). Polyion complexes between ANT1 and PEI according to a literature protocol [19] produce antisense effects, in assays (21) and (22). When 10 μg of ANT1 and 10 μg of PEI are mixed (assay 21), E_{GFP} was reduced to 70%. This means that the same antisense effect is present in the presence of PEI to some extent. However, when PEI is increased to 25 μg (assay 22), the solution becomes more turbid than assay 21 and E_{GFP} increases. PEI is known as an AN ODN carrier; however, poor solubility is a problem [19,20]. The present work confirms this problem in PEI and shows the superiority of s-SPG as an AN ODN carrier.

3.3. Nuclease protection mechanism

Fig. 3 compares E_{GFP} when Exonuclease I was intentionally added to the Promega *E. coli* T7 S30 extract solution. Results show that E_{GFP} is unchanged for the complex (indicated by "protection by s-SPG" in the figure). On the other hand, it is increased for naked ANT1. Since Exonuclease I specifically hydrolyzes DNA single-chains, ANT1 suffers serious hydrolysis when Exonuclease I is added, accounting for E_{GFP} increase with the addition. It is interesting that there is no difference in E_{GFP} when Exonuclease I is added to the ANT1/s-SPG complex. This feature suggests that ANT1 is protected from nuclease hydrolysis by the complex.

To examine how the s-SPG complex protects bound AS ODNs, we performed on antisense assay in a nuclease-free *E. coli* T7 S30 extract solution. Novagen's *E. coli* T7 S30 extract solution is available for linear DNAs and PCR products, which means it must be practically nuclease-free or inhibited [15]. The assay results are presented in Fig. 4. Here, we used the same

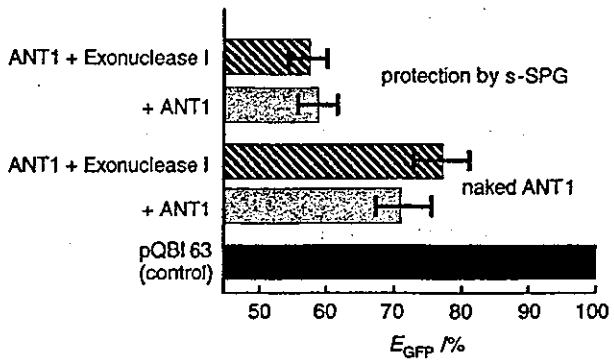

Fig. 3. Comparison of GFP expression efficiency (E_{GFP}) between the ANT1/s-SPG complex and naked ANT1 when Exonuclease I was added to the standard.

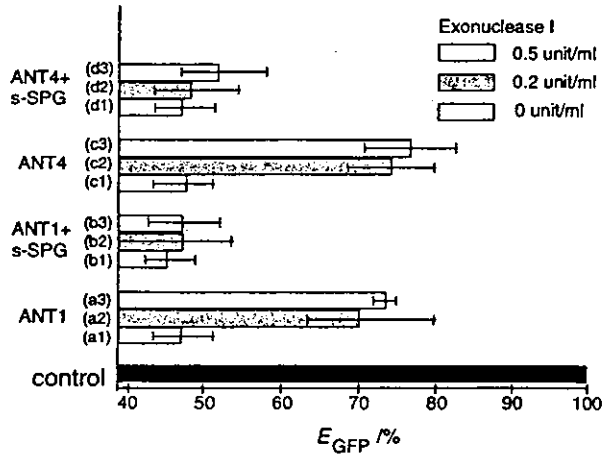

Fig. 4. Effect of addition of Exonuclease I on E_{GFP}, comparing naked ANT and the ANT/s-SPG complexes. Control: pQBI template DNA in Novagen's *E. coli* T7 S30 extract solution. 0.2 and 0.5 unit/ml Exonuclease I was added to the naked ANT1: (assays a2, a3), to naked ANT4: (assays c2, c3), to the s-SPG/ANT1 complex: (assays b2, b3) and to the s-SPG/ANT2 complex: (assays d2, d3).

conditions as those of Figs. 2 and 3, except for using ANT4 and Novagen's *E. coli* T7 S30 extract solution. When Exonuclease I was not present the values for E_{GFP} are almost identical for naked ANTs and their complexes (assays (a1), (b1), (c1) and (d1)). This feature is different from results in Fig. 2, confirming that Novagen's *E. coli* T7 S30 extract solution is practically nuclease activity-free. When Exonuclease I was added to the system, E_{GFP} is increased for the naked ANTs: (assays (a2, a3) and (c2, c3)) as expected. On the other hand, E_{GFP} is unchanged by addition of Exonuclease I for the complex: (assays (b2, b3) and (d2, d3)). These results support that the s-SPG complex protects the bound AS ODNs to a great extent.

ANT1 has the poly(dA) tail at the 3′ end, while ANT4 has this tail at the 5′ end. Exonuclease I hydrolyzes single strand DNA from the 3′ end. Therefore, when exposed to Exonuclease I, ANT4 is expected to be more susceptible to hydrolysis and inactivation than ANT1. In fact, when Fig. 4 assays (a1–a3) are compared with (c1–c3) carefully, E_{GFP} is increased more for the naked ANT4 than naked ANT1. This difference is ascribed to that position difference of the antisense vs. poly(dA) sequence. Additionally, we have evidence to prove that a stable complex is formed between poly(dA) and s-SPG [17], and that the short antisense sequence itself (see Table 1) does not bind specifically to s-SPG. However, for the ANT-poly(dA) fused DNA we do not know whether the hetero sequence component of ANT1 or ANT4 is involved in the complex. If the hetero sequence (i.e., antisense part) is not involved in the complex, it should be more vulnerable than the poly(dA) tail to nuclease digestion In particular, the antisense sequence

located at 3′ end of ANT4 should be the most vulnerable part because Exonuclease I hydrolyzes from this end. However, no significant difference in E_{GFP} is observed between ANT1 + s-SPG and ANT4 + s-SPG(see Fig. 3 assays (b1–b3) and (d1–d3)). One explanation is that the protective s-SPG complexed close to the heterosequence spatially hinders Exonuclease I approach to the DNA. From only this result, it may be premature to conclude that the heterosequence is involved in the complex between the poly(dA) tail and s-SPG.

To sum the AS ODN protection mechanism proposed for the preset system, Fig. 5 schematically presents our model. Once the AS ODN and s-SPG complex is formed, it protects the bound AS ODN from nuclease attack. Survival of the AS ODN to complex target mRNA is increased, thus inhibitis GFP expression over that observed in the naked AS ODN system. This model supposes that the complexed AS ODN is released form the complex when it meets the target mRNA, which means that the binding constant of s-SPG/AS ODN must be less than that of AS ODM/target mRNA. In fact, we found that takeover reaction from s-SPG/poly(A) to poly(A)/poly(T) can be completed in 20 min, suggesting our hypothesis being right. We have clarified this issue in the related paper [21].

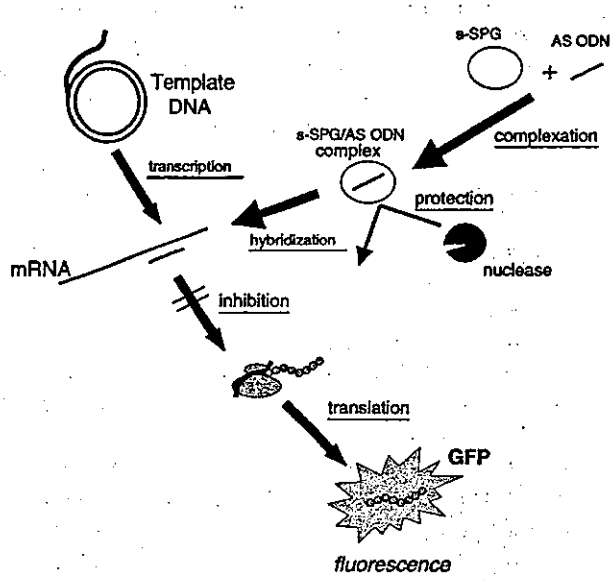

Fig. 5. A schematic illustration to explain the enhanced antisense effect observed in the present system. The template DNA (pQBI63) produces the GFP-coding mRNA by transcription and the mRNA is translated to GFP. When AS ODN (antisense oligonucleotide) is added to this system, the AS ODN binds to the mRNA, inhibiting translation. However, some AS ODNs are hydrolyzed by nuclease. When s-SPG is added to AS ODN, they form a complex. Complexes between AS ODN and s-SPG protect the bound AS ODN from nuclease attack. Levels of intact, surviving AS ODN reaches the target mRNA are increased. This means that inhibition of GFP expression is more enhanced than for the naked AS ODN system.

4. Concluding remarks

We conclude that s-SPG/AS ODN complexes are useful as antisense DNA carriers to reduce nuclease-mediated hydrolysis. We successfully demonstrate that AS ODNs in the s-SPG complex exhibit reduced GFP expression efficiency (or higher antisense effects) than that of naked DNA. When Exonuclease I, which specifically hydrolyzes single DNA chains, was present in the assay system antisense effects are unchanged for the complexes, but significantly weakened in the naked antisense DNA system.

Acknowledgements

This work is financially supported by "Organization and Function", PRESTO, and SORST programs in Japan Science and Technology Corporation (JST).

References

[1] Tabata K, Ito W, Kojima T. Ultrasonic degradation of schizophyllan, an antitumor polysaccharide produced by Schizophyllum commune fries. Carbohydr Res 1981;89:121–35.
[2] Norisuye T, Yanaki T, Fujita H. Triple helix of a Schiphyllum commune polysaccharide in aqueous solution. J Polym Sci Polym Phys Ed 1980;18:547–58.
[3] Yanaki T, Norisuye T, Fujita H. Triple helix of Schizophyllum commune polysaccharide in dilute solution. 3. hydrodynamic properties in water. Macromolecules 1980;13:1462–6.
[4] Sato T, Sakurai K, Norisuye T, Fujita H. Triple helix of Schizophyllum commune polysaccharide in dilute solution. Part VI. Collapse of randomly coiled schizophyllan in mixtures of water and dimethylsulfoxide. Polymer J 1983;15:87–96.
[5] McIntire TM, Brant DA. Observation of the (1→3)-b-D-glucan liner triple helix to macrocycle interconversion using non-contatct atomic force microscopy. J Am Chem Soc 1998;120:6909–19.
[6] Sakurai K, Shinkai S. Molecular recognition of adenine, cytosine, and uracil in a single-stranded RNA by a natural polysaccharide: schizophyllan. J Am Chem Soc 2000;122(18):4520–1.
[7] Sakurai K, Mizu M, Shinkai S. Polysaccharide-polynucleotide complexes. 2. Complementary polynucleotide mimic behavior of the natural polysaccharide schizophyllan in the macromolecular complex with single-stranded RNA and DNA. Biomacromolecules 2001;2(3):641–50.
[8] Mizu M, Koumoto K, Kimura T, Sakurai K, Shinkai S. Protection of polynucleotides from nuclease-mediated hydrolysis by forming a complex with schizophyllan. The preceding submission.
[9] Chalfie M, Tu Y, Euskirchen G, Ward WW, Prasher DC. Green fluorescent protein as a marker for gene expression. Science 1994;263:802–5.
[10] Technical data in Takara manual of GFP, BFP vectors, 2000 (Japanese).
[11] AFPs™ AutoFlouresence Proteins, AFP-Manual (version AFP11-No98), 2001.
[12] Promega, Part# TB219. *E. coli* T7 S30 extract system for circular DNA, 2002.

[13] Murata M, Kaku W, Anada T, Soh N, Katayama Y, Maeda M. Thermo responsive DNA/polymer conjugate for intelligent antisense strategy. Chem Lett 2003;32:266–7.
[14] Anada T, Kano T, Kaku W, Katayama Y, Maeda M. Functional regulation of biomolecule using DNA conjugate. Nucleic Acid Res Suppl 2002;2:269–70.
[15] Novagen EcoPro™ System TB278 06.
[16] 2000 Novagen Catalog. p. 180, http://www.novagen com.
[17] Mizu M, Kimura T, Koumoto K, Sakurai K, Shinkai S. Thermally induced conformational-transisiton of polydeoxyadenosine in the complex with schizophyllan and the base-length dependence of its stability. Chem Commun 2001;429–30.
[18] Atale for four systems, optimized gene expression with the T7 sample system. Promega Note. Number 80, 2002.
[19] Boussif O, Lezoualc'h F, Zanta MA, Mergny MD, Scherman D, Demeneix B, Behr JP. A versatile vector for gene and oligonucleotide transfer into cells in culture and in vivo: polyethylenimine. Proc Natl Acad Sci USA 1995;92:7297–301.
[20] Chirila TV, Rakoczy PE, Garrett KL, Lou X, Constable IJ. The use of synthetic polymers for delivery of therapeutic antisense oligodeoxynucleotides. Biomaterials 2002;23(2):321–42.
[21] Koumoto K, Mizu M, Sakurai K, Kunitake T, Shinkai S. Intelligent release of the single-stranded DNA bound in the schizophyllan complex. Chem Biodiversity, submitted.

Polysaccharide/Polynucleotide Complexes

Part 6

Complementary-Strand-Induced Release of Single-Stranded DNA Bound in the Schizophyllan Complex

by **Kazuya Koumoto**[a]), **Masami Mizu**[a]), **Kazuo Sakurai***[a]), **Toyoki Kunitake**[a]), and **Seiji Shinkai***[b])

[a]) Department of Chemical Processes and Environments, Faculty of Environmental Engineering, The University of Kitakyushu, 1-1 Hibikino, Wakamatsu-ku, Kitakyushu, Fukuoka 808-0135, Japan. (Phone: +81-93-695-3298; fax: +81-93-695-3390; e-mail: sakurai@env.kitakyu-u.ac.jp)

[b]) Department of Chemistry and Biochemistry, Graduate School of Engineering, Kyushu University, Fukuoka 812-8581, Japan.

Spectroscopic properties of single-stranded DNA/schizophyllan ternary complexes (ss-DNA·2s-SPG), induced by addition of either complementary or noncomplementary strands, have been investigated. The addition of the complementary strands to ss-DNA·2s-SPG induced the quick release of the bound ss-DNA to the complementary strands (both DNA and RNA), whereas the ternary complex was unaffected upon addition of noncomplementary strands. Our experiments imply that SPG has complexation properties indispensable to the gene carriers. As far as we know, there is no report on exploitation of such nonviral gene carriers that can accomplish an intelligent release of the bound ss-DNA toward the complementary strands. We believe, therefore, that SPG, a natural and neutral polysaccharide, has a great potential to become a new ss-DNA carrier.

Introduction. – Schizophyllan (SPG) is an extracellular polysaccharide produced by the fungus *Schizophyllum commune*. The main chain of SPG consists of β-1,3-glucan, and every third glucose unit has a β-1,6-glucosidic side chain [1][2]. The three chains are twisted together to form a triple helix (t-SPG) in H_2O, in which strong H-bonds among the 2-OH groups are formed in the main chain [3–6]. It is known that the t-SPG chain dissociates into a single chain of SPG (s-SPG), when dissolved in a denaturing solvent such as dimethylsulfoxide (DMSO) [7][8], and that the triple-helical structure can be restored by exchanging DMSO for H_2O (*Fig. 1*) [9–11]. Such a unique property has been made use of in the food and pharmaceutical industry, and for other purposes [12–14].

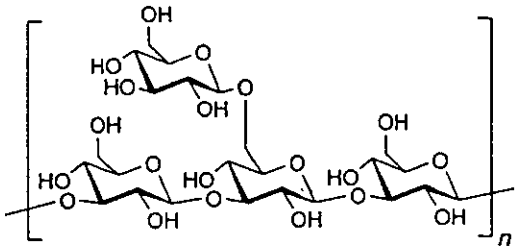

Schizophyllan

Recently, we found that when the renaturation process is carried out in the presence of certain single-stranded (ss) polynucleotides, s-SPG forms macromolecular com-

plexes with the polynuclotides, as schematically shown in *Fig. 1* [15]. Interestingly, the complex dissociates in a cooperative manner upon heating, as if the polysaccharide chain lacking any nucleobase behaves as the complementary strand [15][16]. In addition, taking into consideration that *1*) these complexes possess different melting temperatures [17] and *2*) the minimum base length of polynucleotides to form complexes is different in each nucleobase [17][18], it is clear that the H-bonding interaction between polysaccharides and nucleobases plays an important role in complex formation [16]. To the best of our knowledge, this is the first time that specific interactions between neutral polysaccharides and polynucleotides has been evidenced experimentally. Our further studies have clarified some of the novel properties on the complex: *1*) polysaccharides possessing the β-1,3-glucan main-chain structure can form similar complexes [19][20]; *2*) according to stoichiometric studies, the complex consists of one polynucleotide chain and two polysaccharide chains [16]; and *3*) the polynucleotide chain bound in the complex is resistant against enzymatic hydrolysis [21].

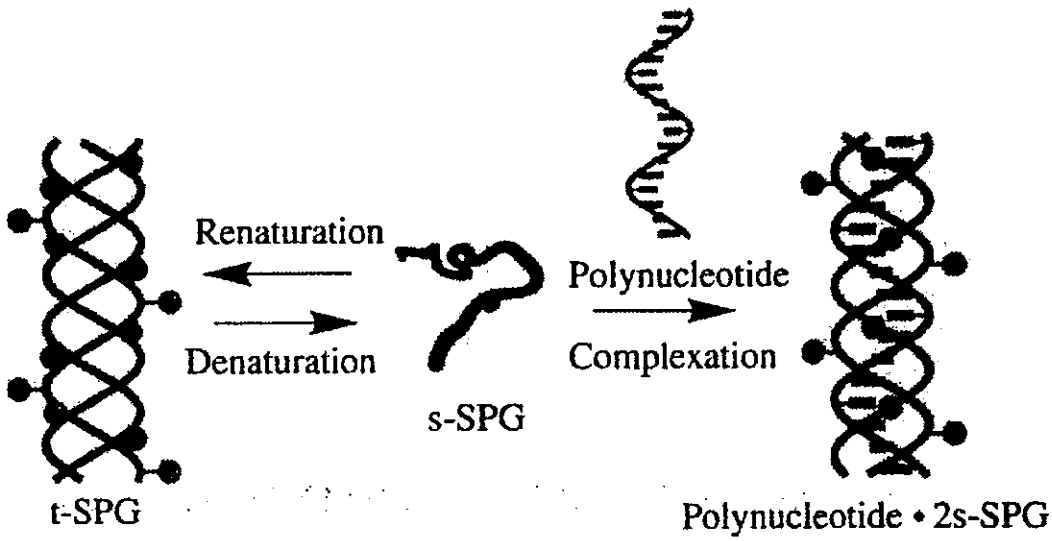

Fig. 1. *Schematic illustration of the equilibria involved in the formation of the triple-helical complex between a polynucleotide and schizophyllan* (s-SPG)

Complex formation and dissociation can be controlled either by changing the pH of the medium [22] or the ion species [23]. These properties are expected to be favorable for industrial or biological applications such as gene separation and gene carriers. To exploit the ability of these complexes as gene carriers, we added the complementary strand to the ss-DNA/s-SPG complex (ss-DNA · 2s-SPG) and observed the spectroscopic changes induced by the addition of the complementary strands. For the peptide nucleic acids (PNA) reported by *Nielsen* and co-workers [24–26], it is known that the incorporation of PNA into double-stranded DNA induces the displacement of the strands, resulting in the formation of DNA · PNA hybrids. In comparison to PNA, the interaction between SPG and DNA (or RNA) is weaker, because the polysaccharide does not provide any *Watson–Crick* or *Hoogsteen* base pairing. It is expected,

therefore, that the addition of the complementary strands to the ss-DNA·2s-SPG complex would induce properties different from those of the PNA and DNA systems.

Results and Discussion. – *Relationship between Circular-Dichroism* (CD) *Spectra and DNA Conformation.* In this study, we chose the poly(dA·2s-SPG) complex as a model system because *1*) the complex has the highest melting temperature among the ss-polynucleotide·2s-SPG complexes ($T_m = 74°$, [NaCl] = 150 mM) [27] and, therefore, is considerably stable under physiological conditions, and *2*) the CD spectra of poly(dA) change drastically upon complexation with s-SPG [18][27]. These properties should make it easy to observe the spectroscopic changes induced by the addition of the complementary strands to ss-DNA·2s-SPG. In general, it is rather difficult to judge duplex formation only from a change in the corresponding CD spectra. Therefore, we first evaluated the relationship between the CD spectral change in the poly(dA)/poly(dT) system and their conformation by both UV and fluorescence spectroscopy. In *Fig. 2, a*, the CD spectral changes upon duplex formation, induced by NaCl, of a mixture of poly(dA) and poly(dT) are shown. At NaCl concentrations lower than 3 mM, the CD spectrum showed only two bands, a positive one at 280 nm, and a negative band at 247 nm. With increasing NaCl concentration, the CD spectra drastically changed: the negative 247-nm band became more intense, and two new maxima appeared at 257 and 263 nm, respectively. We plotted the CD intensity of the characteristic 247-nm band (Θ_{247}) against the NaCl concentration, as shown in *Fig. 2, b*. As can be seen, there is a strong decrease in Θ_{247} at 3–5 mM NaCl concentration, and then a plateau is reached above 5 mM.

In order to assign the above CD spectral changes, we also recorded UV spectra at varying NaCl concentrations. As shown in *Fig. 2, c*, the UV absorbance decreased with increasing NaCl concentration, which can be ascribed to a hypochromic effect due to duplex formation. This absorbance change also supports the view that poly(dA) and poly(dT) form the duplex at NaCl concentrations above *ca.* 5 mM.

Fluorescence spectroscopy is another useful technique to evaluate duplex formation. For example, ethidium bromide can intercalate into a poly(dA·dT) duplex, giving rise to strong fluorescence ($\lambda_{ex} = 330$ nm, $\lambda_{em} = 590$ nm). In *Fig. 2, d*, the relative fluorescence intensity of ethidium bromide/poly(dA)/poly(dT) as a function of the NaCl concentration is shown. Enhancement of the fluorescence intensity I_F was observed at NaCl concentrations higher than 5 mM, before the intensity gradually decreased with increasing NaCl concentration. This decrease in fluorescence intensity observed at high NaCl concentration is due to the decrease in the binding constant between ethidium bromide and poly(dA·dT), as shown by *Maiti* and co-workers [28]. All together, these findings reveal that poly(dA) and poly(dT) form the duplex at NaCl concentrations higher than *ca.* 5 mM. Under the same conditions, the CD spectra showed a synchronized change, which prompted us to conclude that CD spectroscopy is well-suited to follow duplex formation between poly(dA) and poly(dT).

Takeover Reaction of poly(dA) from the s-SPG Complex to poly(dT). These experiments were performed at a NaCl concentration of 150 mM, which is close to physiological conditions. In *Fig. 3, a*, two possible scenarios are shown schematically when poly(dT) is added to poly(dA·2s-SPG): *1*) takeover reaction of the poly(dA) chain from the s-SPG complex to poly(dT) under poly(dA·dT) duplex formation, or

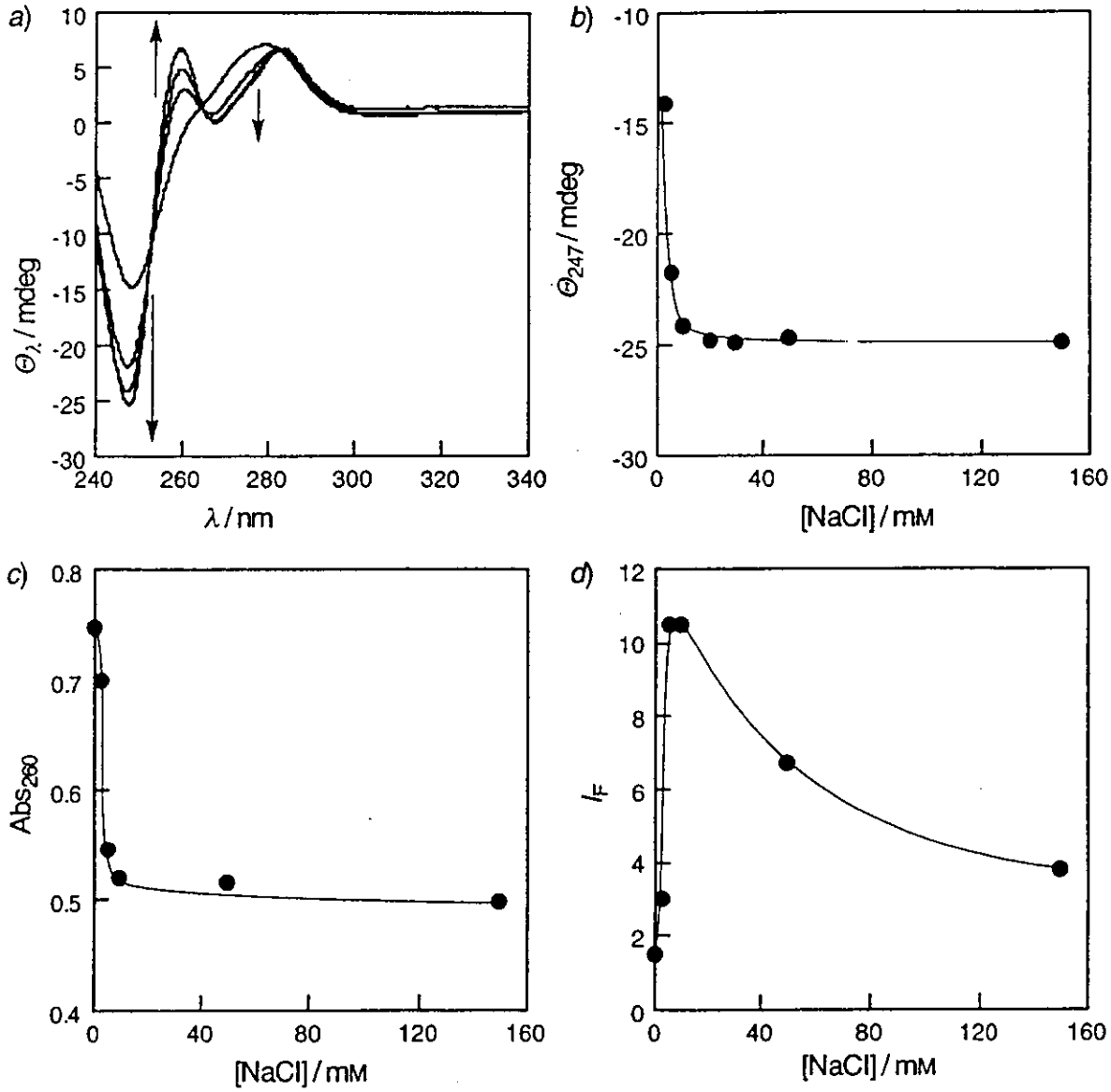

Fig. 2. *Influence of NaCl concentration on the spectral properties of mixtures of poly(dA) and poly(dT).* a) *CD Spectra* (3–150 mM NaCl); b) *plot of the CD ellipticity at 247 nm* (Θ_{247}) vs. *NaCl concentration*; c) UV/VIS absorbance (Abs) *at 260 nm*; d) *relative fluorescence intensity* (I_F) *at an emission wavelength of 590 nm.* Conditions: [Poly(dA)] = [poly(dT)] = 37 μM/repeating unit; T = 37°.

II) retention of the triple-helical complex despite addition of poly(dT). In the first case, the CD spectrum of poly(dA · 2s-SPG) should change to that of poly(dA · dT) (solid line in *Fig. 3, b*), whereas, in the second case, a spectral change from poly(dA · 2s-SPG) to the averaged CD spectrum of the poly(dA · 2s-SPG)/poly(dT) mixture (dotted line in *Fig. 3, b*), is expected.

The experimentally observed CD spectral changes upon addition of poly(dT) to poly(dA · 2s-SPG) at 37° are shown in *Fig. 3, c*. Before the addition of poly(dT) (broken lines), the CD spectrum was identical with that for poly(dA · 2s-SPG) [18], confirming that the complexation was complete. Immediately after the addition of poly(dT), the

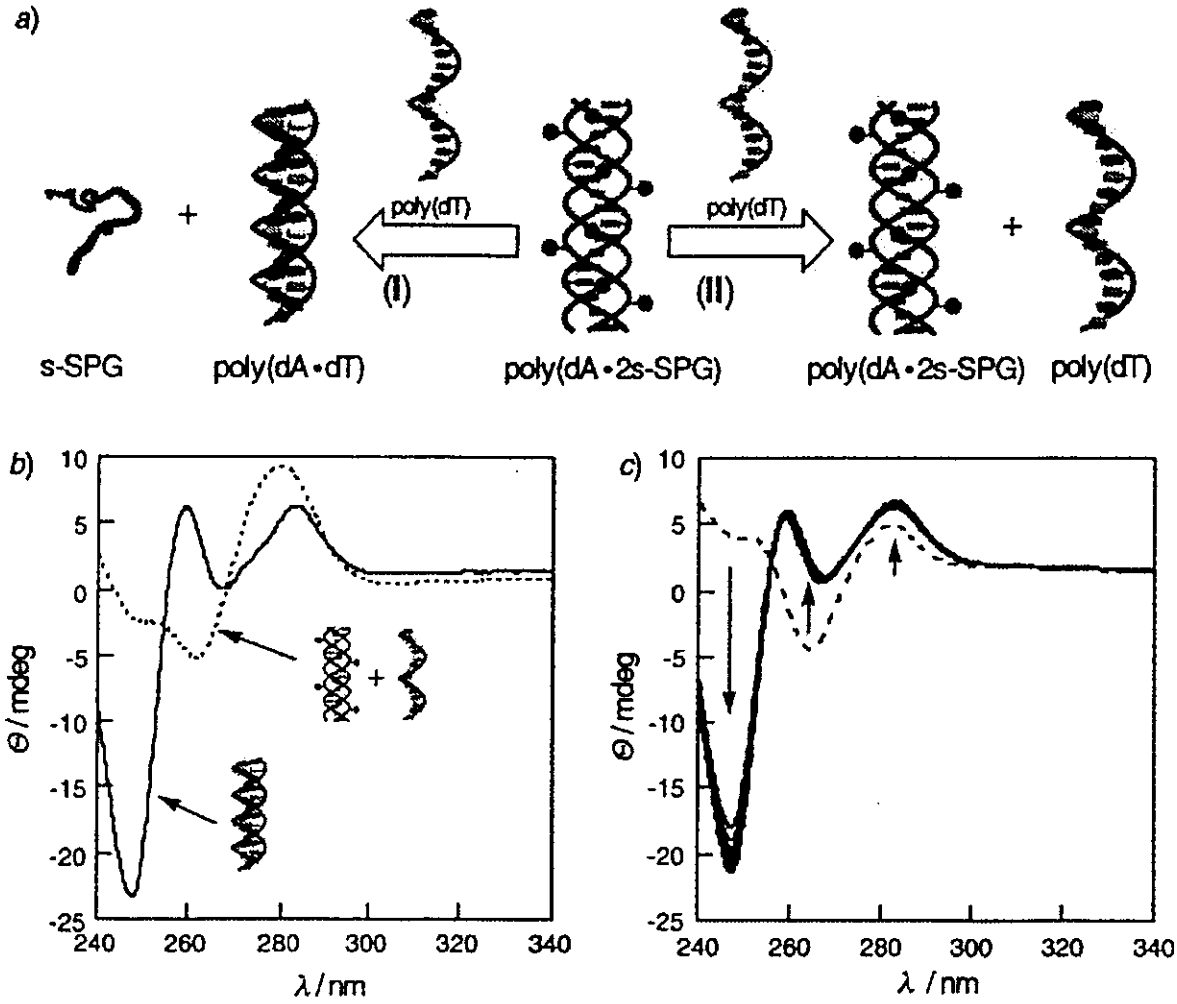

Fig. 3. a) *Schematic illustration of two possible scenarios upon addition of poly(dT) as the complementary strand to poly(dA)·2s-SPG.* b) *CD Spectrum of poly(dA·dT)* (solid line) *and calculated CD spectrum of the mixture of poly(dA)·2s-SPG and poly(dT)* (dotted line). c) *Time-dependent CD spectral changes after addition of poly(dT) to poly(dA)·2s-SPG.* Broken line: before addition of poly(dT); solid lines: CD spectra taken in 10-min intervals after addition of poly(dT). Conditions: [poly(dA)] = [poly(dT)] = 37 μM/repeating unit; [s-SPG] = 25 μM/repeating unit. [3]

spectrum changed drastically, indicating formation of poly(dA·dT). The takeover reaction occured so quickly that the initial change could not be followed (*ca.* 75% of poly(dT) had been hybridized with poly(dA) within 1 min).

Next, we evaluated salt effects. In *Fig. 4*, the change in CD ellipticity, $-\Delta\Theta_{247}$, is plotted against reaction time for various NaCl concentrations. Here, $-\Theta_{247}$ is defined by subtracting the calculated CD ellipticity of the mixture of poly(dA·2s-SPG) and poly(dT) proper from that at a given reaction time. At 3-mM NaCl concentration, the hybridization between poly(dA) and poly(dT) cannot take place owing to the large repulsion between the phosphate anions, so that there was no increment in $-\Delta CD_{247}$, in contrast to higher NaCl concentrations. Judging from these experiments, it is obvious that the takeover reaction commonly takes place whenever poly(dA) forms a duplex with poly(dT).

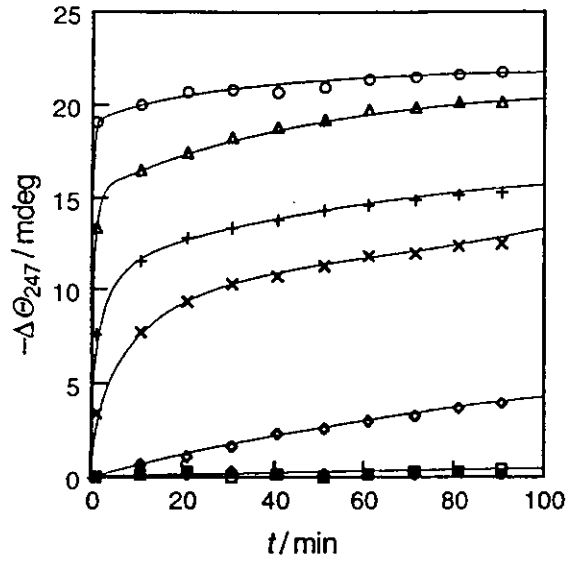

Fig. 4. *Influence of NaCl concentration on the takeover reaction after addition of poly(dT) to poly(dA)·2s-SPG.* The process was monitored by the change in the diagnostic CD ellipticity $\Delta\Theta_{247}$ as a function of time at the following NaCl concentrations: 3 (◆), 5 (□), 10 (◇), 20 (×), 30 (+), 50 (△), and 150 mM (○). The term $-\Delta\Theta_{247}$ was obtained by subtracting the calculated CD ellipticity Θ_{247} of the mixture of poly(dA)·2s-SPG and poly(dT) from that recorded at a given reaction time. Conditions: [poly(dA)] = [poly(dT)] = 37 μM/repeating unit; [s-SPG] = 25 μM/repeating unit.

The above takeover reaction can also be detected by means of fluorescence spectroscopy. In *Fig. 5*, the relative fluorescence intensity change at 590 nm after addition of poly(dT) to poly(dA·2s-SPG) at 10-mM NaCl concentration in the presence of ethidium bromide (2.4 μg/ml) is shown. At this salt concentration, the

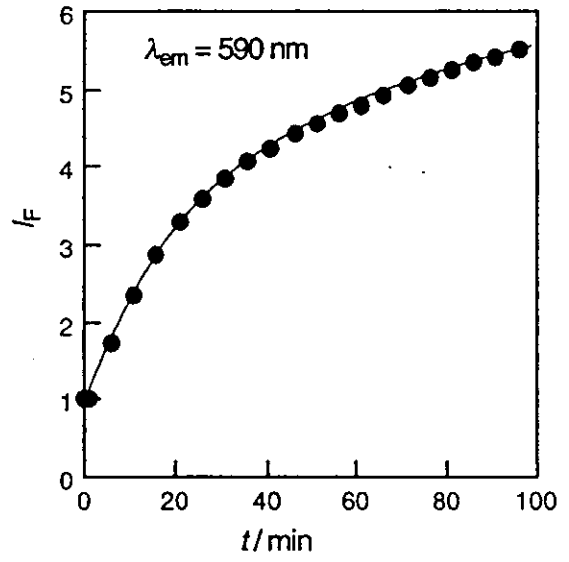

Fig. 5. *Change in relative fluorescence intensity (I_F) at an emission wavelength of 590 nm* (excitation: 330 nm) *after addition of poly(dT) to poly(dA)·2s-SPG.* Conditions: [poly(dA)] = [poly(dT)] = 37 μM/repeating unit; [s-SPG] = 25 μM/repeating unit; [ethidium bromide] = 2.4 μg/ml.

change in relative fluorescence intensity due to intercalation is highest (see *Fig. 2, d*). As shown in *Fig. 5*, the relative fluorescence intensity increased after addition of poly(dT), the trend being similar as in the CD spectral analysis.

Takeover Reaction in Other Systems. As mentioned above, poly(dA·2s-SPG) can release the bound poly(dA) from the s-SPG complex *via* hybridization (duplex formation with poly(dT)). We, therefore, tested whether the takeover reaction can also take place in other systems. We used poly(dT·2s-SPG) instead of poly(dA·2s-SPG) and added poly(dA) to the complex; and in a second experiment, the complementary strand was changed from poly(dT) to poly(U) to evaluate the difference between DNA·DNA and DNA·RNA structures.

In *Fig. 6, a*, the time-dependent CD spectral changes of poly(dT·2s-SPG) after addition of poly(dA) at 5° and 150-mM NaCl concentration are shown. The temperature was kept below the melting temperature of poly(dT·2s-SPG) ($T_m = 17°$ at 150-mM NaCl concentration) [29]. As evident from *Fig. 6, a*, the takeover reaction does occur, as in the case of poly(dA·2s-SPG), indicating that in the DNA·DNA system, the takeover reaction occurs in all ss-DNA·2s-SPG complexes. Next, we extended the experiment to a DNA·RNA hybrid system. In *Fig. 6, b*, the time-dependent fluorescence-intensity change of poly(dA)·2s-SPG upon addition of poly(U) is shown ($T = 37°$, [NaCl] = 50 mM)[1]. The relative fluorescence intensity started to increase after addition of poly(U) to poly(dA·2s-SPG), indicating that the takeover reaction of

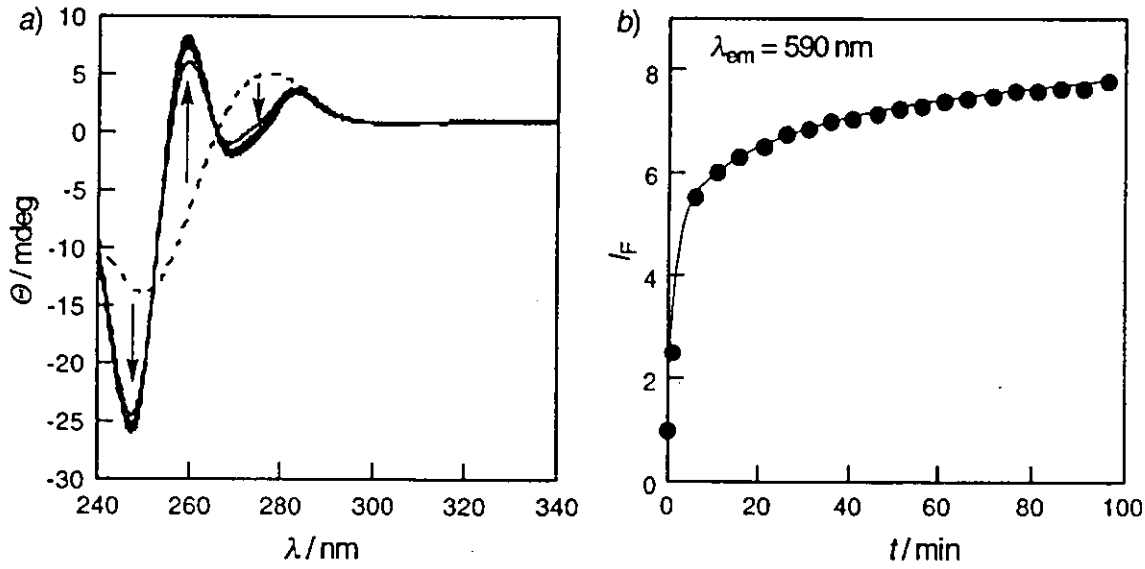

Fig. 6. *Time-dependent CD spectral changes recorded in 10-min intervals after addition of poly(dA) to poly(dT)·2s-SPG* ($T = 5°$; [NaCl] = 150 mM). b) *Change in relative fluorescence intensity* (I_F) *at an emission wavelength of 590 nm* (excitation: 330 nm) *after addition of poly(U) to poly(dA)·2s-SPG* ($T = 37°$; [NaCl] = 50 mM; [poly(dA)] = [poly(dT)] = [poly(U)] = 37 μM/repeating unit; [s-SPG] = 25 μM/repeating unit; [ethidium bromide] = 2.4 μg/ml).

[1]) According to UV- and fluorescence-spectroscopic analyses, poly(dA) forms the duplex with poly(U) at NaCl concentrations above 10–50 mM, and the highest fluorescence intensity change occurs at a NaCl concentration of *ca.* 50 mM (data not shown).

the ss-DNA bound in the s-SPG complex to the complementary strand can be applied to both DNA and RNA systems.

Addition of Noncomplementary Strand to Poly(dA·2s-SPG). In order to confirm the nucleobase specificity of the takeover reaction, we next added a noncomplementary strand, poly(dC), to poly(dA·2s-SPG) and performed a spectroscopic analysis. Here, the following two scenarios are possible (*Fig. 7, a*): *I*) the added poly(dC) induces dissociation of the ternary complex, or *II*) the complex remains unaffected. In case *I*, the CD spectrum should change to the dotted line in *Fig. 7, b* (averaged spectra of poly(dC) and poly(dA)). In case *II*, the CD spectrum should change to the solid line in *Fig. 7, b* (averaged spectra of complex and poly(U)). In *Fig. 7, c*, the time-dependent CD spectral changes, observed when poly(dC) was added to poly(dA·2s-SPG), are shown, revealing that the CD spectra change to those of the mixture of poly(dA·2s-

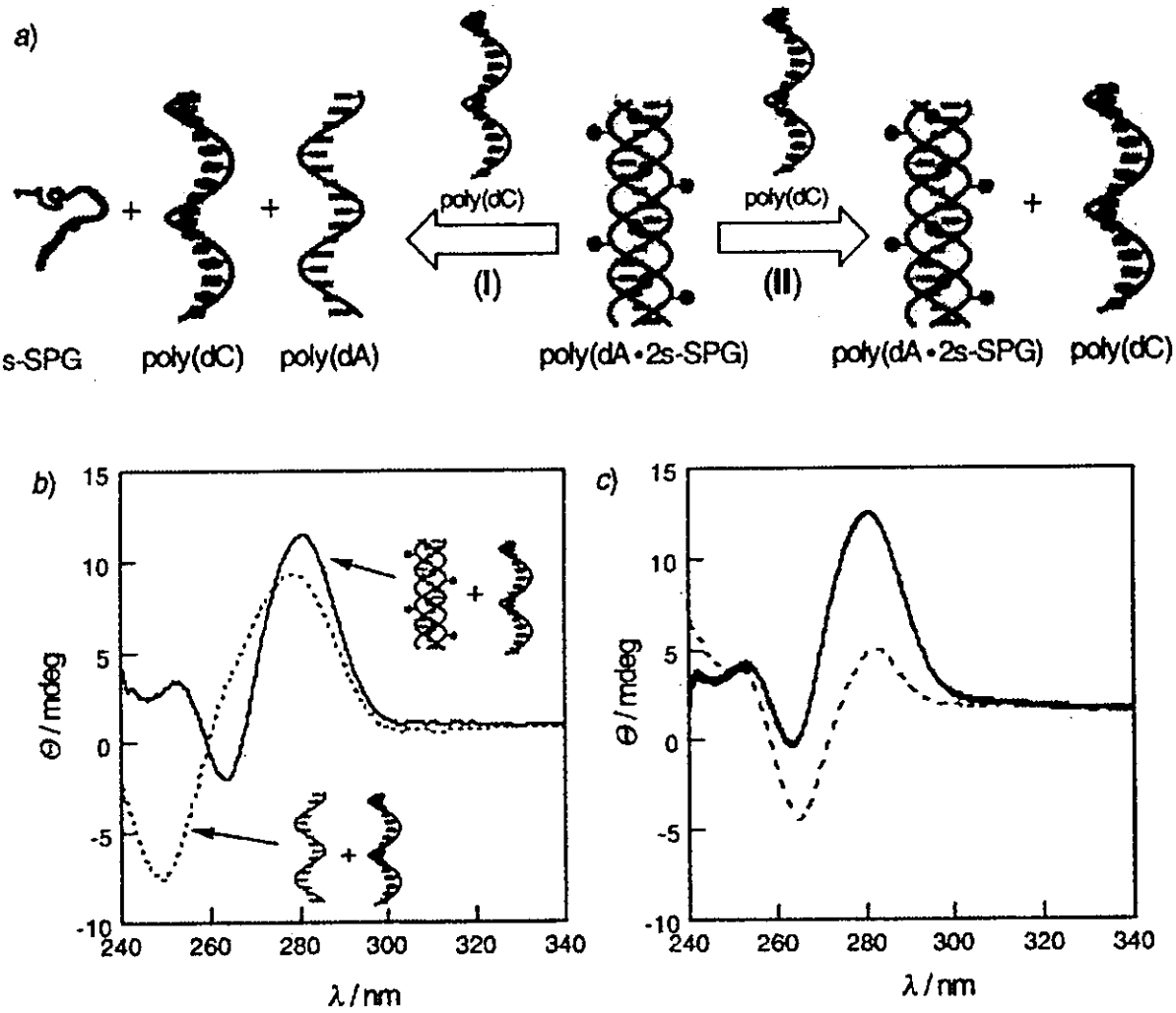

Fig. 7. a) *Schematic illustration of two possible scenarios upon addition of poly(dC) as a noncomplementary strand to poly(dA)·2s-SPG.* b) *Calculated CD Spectra of the mixtures of poly(dA)·2s-SPG and poly(dC)* (solid line) vs. *poly(dA) and poly(dC)* (dotted line). c) *Time-dependent CD spectral changes* (solid lines) *recorded in 10-min intervals after addition of poly(dC) to poly(dA)·2s-SPG.* Broken line: before addition of poly(dC). Conditions: [poly(dA)] = [poly(dC)] = 37 μM/repeating unit; [s-SPG] = 25 μM/repeating unit.

SPG) and poly(dC). A similar behavior, *i.e.*, that addition of a noncomplementary strand does *not* induce the dissociation of the s-SPG complexes, was also observed for poly(C) and poly(G).

Conclusions. – From the foregoing results, one can conclude that the ss-DNA · 2s-SPG complex releases the bound ss-DNA only when the complex meets the complementary strand, otherwise the ternary complex remains intact. Although there have been many reports on the exploitation of such nonviral carriers, this is the first experimental evidence that this polysaccharide/polynucleotide complex selectively releases the bound ss-DNA to the complementary strand. Therefore, we believe that SPG will eventually become a new ss-DNA carrier, with potential applications in antisense therapy. In addition, we can point out the nontoxic nature of schizophyllan as a great advantage of this hybrid system.

We thank *Taito Co.* (Japan) for providing the schizophyllan samples. *K. K.* is indebted to the *Japan Society for the Promotion of Science* (*JSPS*) for financial support. This research has been conducted with financial support from the JST SORST program.

Experimental Part

General. t-SPG (M_w = 450,000; degree of polymerization (DP): 230) was kindly supplied by *Taito Co.*, Japan. The polynucleotides poly(C), poly(U), poly(dA), and poly(dT) (DPs *ca.* 570, 400, 300, and 260, resp.) were purchased from *Amersham Pharmacia*, and poly(G) (DP *ca.* 300) from *Sigma*. RNase-Free, deionized and distilled H_2O was used for all experiments. DMSO and aq. ethidium-bromide soln. (10 mg/ml) were purchased from *Kishida Chemicals* and *Nippon Gene*, Japan, resp. All chemicals were used without further purification. UV/VIS and Fluorescence spectra were recorded on a *Jasco-V-570-UV/VIS/NIR* spectrometer and on a *Hitachi-F-4500* fluorescence spectrophotometer, resp., in thermostated 1-cm quartz cells. Circular dichroism (CD) spectra were recorded on a *Jasco-J-820KS* spectropolarimeter in the range of 240–340 nm, with 1-cm quartz cells equipped with a H_2O-jacket to control the cell temp.

Sample Preparation. All samples were prepared by adding a DMSO s-SPG soln. to an aq. soln. of the polynucleotide, such that the H_2O content (volume fraction) of the H_2O/DMSO mixture was 92% (see [16][17]). The samples thus obtained were equilibrated (to allow for tripple-helical complex formation) at a temp. of 4° for at least 3 d, before measurements were made. The final conc. per polypeptide repeating unit was 37 μM each for poly(dA), poly(dT), poly(dC), poly(C), poly(G), and poly(U). The s-SPG conc. was 25 μM, and that of ethidium bromide 6.1 μM (2.4 μg/ml).

REFERENCES

[1] S. Kikumoto, T. Miyajima, S. Yoshizumi, S. Fujimoto, K. Kimura, *J. Agric. Chem. Soc. Jpn.* **1970**, *44*, 337.
[2] S. Kikumoto, T. Miyajima, K. Kimura, S. Okubo, N. Komatsu, *J. Agric. Chem. Soc. Jpn.* **1970**, *45*, 162.
[3] Y. Deslandes, R. H. Marchessalut, A. Sarko, *Macromolecules* **1980**, *13*, 1466.
[4] T. L. Bluhm, A. Sarko, *Can. J. Chem.* **1977**, *55*, 293.
[5] C. T. Chuah, A. Sarko, Y. Deslandes, R. H. Marchessault, *Macromolecules* **1983**, *16*, 1375.
[6] T. L. Bluhm, Y. Deslandes, R. H. Marchessault, S. Perez, M. Rinaudo, *Carbohydr. Res.* **1982**, *100*, 117.
[7] T. Yanaki, T. Norisuye, H. Fujita, *Macromolecules* **1980**, *13*, 1462.
[8] T. Norisuye, T. Yanaki, H. Fujita, *J. Polym. Sci., Part B: Polym. Phys.* **1980**, *18*, 547.
[9] T. M. McIntire, R. M. Penner, D. A. Brant, *Macromolecules* **1995**, *28*, 6375.
[10] T. M. McIntire, D. A. Brant, *J. Am. Chem. Soc.* **1998**, *120*, 6909.
[11] B. H. Falch, B. T. Stokke, *Carbohydr. Polym.* **2001**, *44*, 113.
[12] I. Y. Lee, in 'Biopolymers. Vol. 5: Polysaccharides I – Polysaccharides from Prokaryotes', Eds. E. J. Vandamme, S. De Baets, A. Steinbüchel, J. Wiley & Sons, New York, 2001, p. 135.

[13] I. Giavasis, L. M. Harvey, B. McNeil, in 'Biopolymers. Vol. 6: Polysaccharides II – Polysaccharides from Eukaryotes', Ed. E. J. Vandamme, S. De Baets, A. Steinbüchel, J. Wiley & Sons, New York, 2001, p. 37.
[14] U. Rau, in 'Biopolymers. Vol. 6: Polysaccharides II – Polysaccharides from Eukaryotes', Ed. E. J. Vandamme, S. De Baets, A. Steinbüchel, J. Wiley & Sons, New York, 2001, p. 61.
[15] K. Sakurai, S. Shinkai, *J. Am. Chem. Soc.* **2000**, *122*, 4520.
[16] K. Sakurai, M. Mizu, S. Shinkai, *Biomacromolecules* **2001**, *3*, 641.
[17] K. Koumoto, T. Kimura, M. Mizu, T. Kunitake, K. Sakurai, S. Shinkai, *J. Chem. Soc., Perkin Trans. 1* **2002**, 2477.
[18] M. Mizu, T. Kimura, K. Koumoto, K. Sakurai, S. Shinkai, *Chem. Commun.* **2001**, 429.
[19] T. Kimura, K. Koumoto, K. Sakurai, S. Shinkai, *Chem. Lett.* **2000**, 1243.
[20] K. Koumoto, T. Kimura, H. Kobayashi, K. Sakurai, S. Shinkai, *Chem. Lett.* **2001**, 908.
[21] M. Mizu, K. Koumoto, T. Kimura, K. Sakurai, S. Shinkai, *Biomaterials* **2004**, *25*, 3109.
[22] K. Sakurai, R. Iguchi, M. Mizu, K. Koumoto, S. Shinkai, *Bioorg. Chem.* **2003**, *31*, 216.
[23] K. Sakurai, R. Iguchi, K. Koumoto, T. Kimura, M. Mizu, Y. Hisaeda, S. Shinkai, *Biopolymers* **2002**, *65*, 1.
[24] P. E. Nielsen, M. Egholm, R. H. Berg, O. Buchardt, *Science* **1991**, *254*, 1497.
[25] V. V. Demidov, E. Protozanova, K. I. Izvolsky, C. Price, P. E. Nielsen, M. D. Kamenetskill, *Proc. Natl. Acad. Sci. U.S.A.* **2002**, *99*, 5953.
[26] B. Hyrup, P. E. Nielsen, *Bioorg. Med. Chem.* **1996**, *4*, 5.
[27] M. Mizu, K. Koumoto, T. Kimura, K. Sakurai, S. Shinkai, *Polym. J.* **2003**, *35*, 714.
[28] A. Sen, A. Ray, M. Maiti, *Biophys. Chem.* **1996**, *59*, 155.
[29] Unpublished results.

Received November 6, 2003

First Observation by Fluorescence Polarization of Complexation between mRNA and the Natural Polysaccharide Schizophyllan[1])

by **Ryouji Karinaga**[a]), **Masami Mizu**[a]), **Kazuya Koumoto**[a]), **Takahisa Anada**[a]), **Seiji Shinkai**[b]), **Taro Kimura**[c]), and **Kazuo Sakurai***[a])

[a]) Department of Chemical Process and Environments, The University of Kitakyushu, 1-1, Hibikino, Wakamatu-ku, Kitakyushu, Fukuoka 808-0135, Japan (e-mail: sakurai@env.kitakyu-u.ac.jp)

[b]) Faculty of Engineering Department of Chemistry & Biochemistry, Graduate School of Engineering, Kyushu University, 6-10-1 Hakozaki, Higashi-ku, Fukuoka, Fukuoka 812-8581, Japan

[c]) Fukuoka Industrial Technology Center, Biotechnology and Food Research Institute, 1465-5 Aikawa, Kurume 839-0861, Japan

Schizophyllan is a natural β-(1→3)-D-glucan that exists as a triple helix in H_2O and as a single chain in dimethylsulfoxide (DMSO) or basic solution (pH >13). As we have already reported, when a homopolynucleotide (*e.g.*, poly(dA), poly(A), or poly(C)) is added to a schizophyllan/DMSO solution, and, subsequently, DMSO is exchanged for H_2O, the single chain of schizophyllan forms a complex with the polynucleotide. Since eukaryotic mRNAs have poly(A) tails, we hypothesized that schizophyllan can bind to mRNA by interacting with this tail. However, we have not yet observed complexation between schizophyllan and mRNA after exchanging DMSO for H_2O. In this report, we show that the complexation can be accelerated when the solution pH is changed from 13 to 7–8 in the presence of schizophyllan and polynucleotides. By this approach, we found that schizophyllan forms a complex with a yeast mRNA.

Introduction. – Most eukaryotic mRNAs acquire a poly(A) tail at the 3′ end after post-transcriptional cleavage of the mRNA precursor. The poly(A) tail provides a binding site for some proteins, and the length of the tail determines the mRNA decay rate [2]. Therefore, the poly(A) tail plays an important role in the regulation of gene expression. In recombinant-DNA techniques, the poly(A) tail is essential for isolation of mRNA from total RNA and/or for reverse-transcription of mRNA to cDNA [3][4]. Thus, the biological and technological importance of the poly(A) tail stimulated us to investigate materials that can bind to the poly(A) tail.

Recently, our group found that natural β-(1→3)-D-glucans (*Fig. 1,a*), such as schizophyllan (SPG) and curdlan, can form stoichiometric complexes with synthetic poly(A) (not the mRNA poly(A) tail) as well as other homopolynucleotides [5–7]. The complexation takes place when the glucan is first dissolved in DMSO, and then the glucan/DMSO solution is mixed with sufficient aqueous poly(A) solution, so that the volume fraction of H_2O is ≥ 0.6. The dissolution in DMSO eradicates all higher structures that normally form in aqueous solution, *i.e.*, the triple-helix adopted by β-(1→3)-D-glucans brought about by H-bonding between the C(2)–OH groups of the main-chain glucans [8]. The introduction of H_2O leads to reconstruction or renatura-

[1]) This is the 23rd paper in the series of 'Polysaccharide–Polynucleotide Complexes', and a related work has been presented in the 29th Symposium on Nucleic Acid Chemistry in Japan, using a SPG-appended column to separate mRNA [1].

tion of the triple helix in the absence of poly(A) [9], or to a SPG-poly(A) complex in the presence of poly(A). Complexation from DMSO solution (the DMSO method) has the drawback that it takes a few days to complete the complexation with poly(A) or poly(C), probably because the continued presence of DMSO decreases the stability of the complex [6]. This becomes a serious problem when we attempt to form the complex from mRNA and the β-(1 → 3)-D-glucan, due to the low stability of the complex and poor reproducibility. The renaturation of β-(1 → 3)-D-glucans can alternatively be achieved by changing the solvent pH from basic to acidic conditions (the pH method) [10][11]. Herein, we apply changes in pH to bring about complex formation between mRNA and β-(1 → 3)-D-glucans, and this paper presents the first evidence that the natural neutral glucan specifically forms a complex with a yeast mRNA.

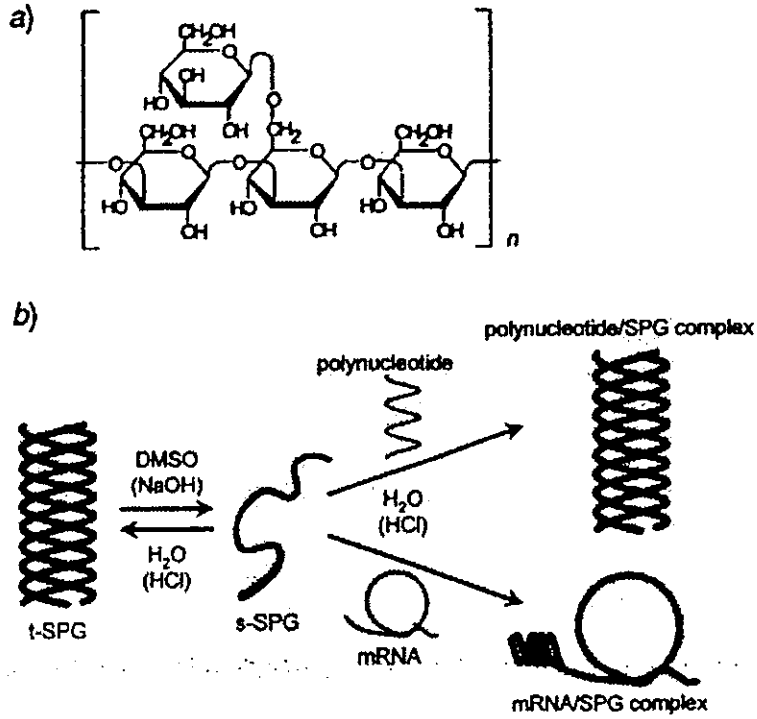

Fig. 1. a) *Chemical structure of the β-(1 → 3)-D-glucan schizophyllan, and* b) *its pH dependent denaturation, renaturation and complexation processes.* The same changes can be induced by DMSO denaturation (see text). Since s-SPG can bind to poly(A), the poly(A) tail in mRNA should also be recognized by s-SPG during renaturation.

Fig. 1, b, illustrates the pH dependency of helix and complex formation. The triple helix of SPG (t-SPG), the most stable conformation at pH 7–8, dissociates to single chains (s-SPG) when dissolved in aqueous NaOH solution at pH 13. After mRNA (or poly(A)) is added to the basic solution, the pH is adjusted to 7–8 by addition of a *Tris*/HCl solution. Since mRNAs contain poly(A) tails, we reasoned that s-SPG may also be able to bind to the tail. We examined the effect of pH on the complexation between synthetic poly(A) (as a model) and s-SPG by circular dichroism (CD) spectroscopy. We found that the CD spectrum is more sensitive to complexation of s-SPG with poly(A) than with mRNA. In fact, it was difficult to observe the complexation between mRNA and s-SPG by CD, presumably because of the relative shortness of the poly(A) tail,

which is no more than 200 base pairs, and only *ca.* 60–90 base pairs in yeast mRNA, *i.e.* less than a few percent of the total composition of mRNA.

Results and Discussion. – *Fig. 2,a* shows the time development of the CD spectrum after the pH is adjusted from 13.0 to 7.0 for the poly(A)/s-SPG system. In this experiment, the number of the repeating units for SPG and poly(A) are 230 and 250, respectively. As time elapses, enhancement of the positive band at 265 nm and the negative band at 248 nm is observed, and the maximum shifts slightly to lower wavelength and the minimum shifts to higher wavelength. All these features indicate that a complex is formed [2b][6], and, importantly, by the pH method, the change in CD is complete after 200 min. When we carried out the similar CD measurements with DMSO as the denaturant with the same salt, *Tris*, poly(A), and s-SPG concentrations at pH 7.0, 2 days passed before a stable CD spectrum was obtained. We define the complex-formation ratio as CD(t)/CD(inf), where CD(t) and CD(inf) are the normalized CD amplitudes at time t (min) and for the stable state at infinite time, respectively, for the positive band at 265 nm. The complex-formation ratio is plotted as a function of the reaction time in *Fig. 2,b*, and demonstrates that the complexation rate is higher for the pH method relative to that of the DMSO method.

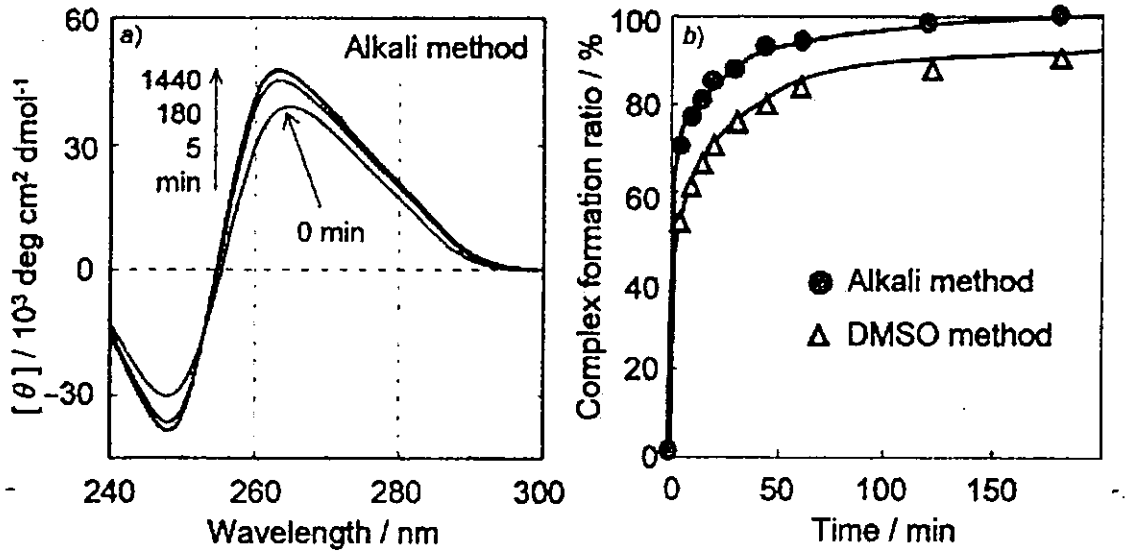

Fig. 2. a) *Development of the CD spectrum during formation of the complex between poly(A) and s-SPG when the complex is made* via *pH change and* b) *comparison of the complex-formation rates under DMSO and pH denaturation/renaturation methods*

A fluorescein moiety can be introduced by reaction of the OH group of the SPG glucose with fluorescein 4-isothiocyanate (FITC) [12]. The reaction conditions were chosen such that one or two fluorescein moieties became attached to each s-SPG molecule (determined by elemental analysis) and, hereafter, this adduct is denoted s-SPG-FITC50. After confirming complexation between poly(A) and s-SPG-FITC50 by gel electrophoresis, we measured the degree of fluorescence polarization (P) [13] in the complexes, comparing the difference between the poly(G) and poly(A) systems (poly(G), which does not form a complex, serves as a control [6]). Subsequently, we

examined mRNA isolated from *Saccharomyces cerevisiae*, compared with a mixture of rRNA and tRNA. The data are summarized in *Fig. 3*, where P is plotted as a function of the polynucleotide/s-SPG molar ratio. Here, P is defined on the basis of the fluorescence intensities parallel (F_{PA}) and perpendicular (F_{PE}) to the excitation plane (*Eqn. 1*).

$$P = \frac{F_{PA} - F_{PE}}{F_{PA} + F_{PE}} \tag{1}$$

Since larger molecules are less mobile, the difference between F_{PA} and F_{PE} (*i.e.*, the denominator of *Eqn. 1*) becomes larger with increasing molecular weight, and the P value increases.

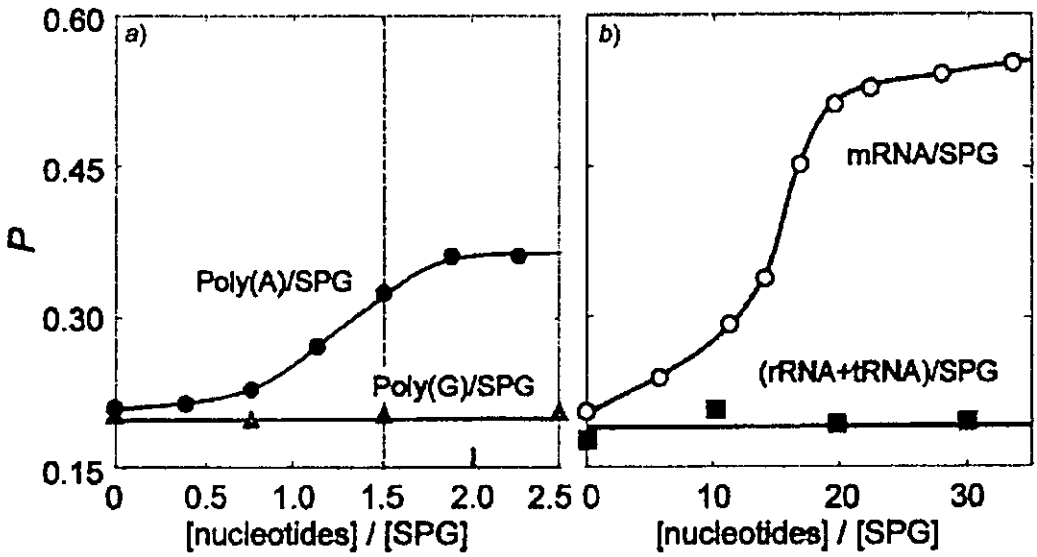

Fig. 3. *Dependence of the fluorescence polarization* (P) *on the concentrations of polynucleotide/s-SPG complexes, comparing* a) *poly(A) with poly(G), and* b) *mRNA with the mixture of rRNA and tRNA.* The s-SPG-FITC50 molar concentrations were fixed at 7.7×10^{-8} M. The s-SPG and polynucleotides samples were first dissolved in 0.25N NaOH and immediately neutralized by adding HCl/*Tris* buffer to obtain solutions at pH 7–8. The vertical dotted line in *a* indicates the stoichiometry of the poly(A)/s-SPG complex.

As plotted in *Fig. 3,a*, the mixtures of poly(G) and s-SPG-FITC50 exhibit a P value of 0.2 essentially independent of the molar ratio, while, for the poly(A) system, P increases with increasing molar ratio, leveling off at 0.36, where the ratio is greater than 2.0. The difference between the poly(G) and poly(A) systems is consistent with the complexation ability of these two polynucleotides. The stoichiometry for the poly(A) complex had already been determined by *Job*-plot analysis to be 1.5 (indicated by the dotted line) [6]. The molar-ratio dependence of P is approximately consistent with the reported stoichiometry. Consequently, the fluorescence polarization for s-SPG-FITC50/polynucleotide quantitatively correlates with complexation ability.

When we examined mRNA and mixtures of tRNA and rRNA, we found that the addition of mRNA increases P with increasing molar ratio, while the other RNAs do not induce any change. These results indicate that a complex forms between s-SPG and mRNA, but not between s-SPG and the other RNAs. This difference in complexation

ability implies that the poly(A) tail of mRNA binds to s-SPG, but that the hetero sequences in the other RNA samples (as well as in the bulk of the mRNA) do not. It should be emphasized that this is the first evidence for the formation of a complex between a natural, neutral polysaccharide and mRNA. Although there are some proteins that can bind to mRNA, most do so by electrostatic interactions. In the present complex, s-SPG is not charged, thus a completely different mechanism must be involved in the complexation [6].

In *Fig. 3,b*, *P* for the mRNA/s-SPG-FITC50 complex levels off at a value (*ca.* 0.55) higher than that of the poly(A) system (0.36), and the leveling-off occurs at the larger molar ratio than that of the poly(A) system. The fluorescence polarization is related to the rotational diffusion coefficient of the dye-bound molecules [13], and the higher *P* indicates a lower coefficient and, generally, a higher molecular weight. Therefore, the higher *P* for mRNA than for poly(A) probably reflects the molecular-weight difference between these species. The higher molar ratio for leveling-off is probably due to binding of only the poly(A) tail to s-SPG while the remainder of the mRNA remains unbound.

To the best of our knowledge, this is the first experimental demonstration of a natural, neutral polysaccharide that is able to bind the mRNA poly(A) tail. Previously, the only species known to bind the poly(A) tail are poly(dT) and positively charged proteins. Therefore, the present finding should open new possibilities to apply this polysaccharide for purification and separation of mRNA from total RNA. Furthermore, in the β-(1 → 3)-D-glucan family, schizophyllan and lentinan have been commercialized as medicines against uterine cancers, however, the detailed molecular mechanisms of their medicinal action have not yet been clarified [14]. The present finding may provide a clue to understanding the biological mechanisms of β-(1 → 3)-D-glucans.

Experimental Part

The schizophyllan (average molecular weight = 15×10^4 Da as the single chain [5][6]) sample was kindly supplied by *Taito Co. Ltd.*, Japan, and poly(A) and poly(G) were purchased from *Amersham Pharmacia*. The degree of polymerization, calculated from the reported sedimentation velocities, were 250 and 300 for poly(A) and poly(G), resp. The mRNA sample used in this study was extracted form *Saccharomyces cerevisiae* Kyokai No. 7, which was kindly supplied by the *Fukuoka Industrial Technology Center, Biotechnology and Food Research Institute*. The yeast cells were cultured in YM medium (*Difco*), and the total RNA was isolated by means of the acid guanidium-phenol-$CHCl_3$ method. From the total RNA, mRNA was purified with the *Oligotex-MAG mRNA Purification Kit* (*TaKaRa*) according to the supplied manual. The concentration of mRNA was determined by UV spectrometry. After extraction of the mRNA, the remaining RNA was used as a mixture of tRNA and rRNA. Flourescein-attached schizophyllan was prepared by adding an extra amount of an acetone soln. of flourescein isothiocyanate (*Dojin*, Japan) to the aq. schizophyllan soln. (1.0 g/dl). We assume that this method modifies mainly the 6-OH group. After precipitation with acetone and washing with toluene several times, the product was freeze-dried. The modification level was determined by UV spectroscopy (based on $\varepsilon = 77000$) to be less than 0.5 mol-%, *i.e.*, *ca.* one of every 200 repeating units bears the flourescein group.

The CD spectra in the 240–300-nm region were measured at 15° on a *Jasco J-720WI* spectropolarimeter with a 1.0-cm cell equipped with a water jacket to control the cell temp. The molecular ellipticity ($[\theta]$) was evaluated by a conventional method. The poly(A) and s-SPG molar concentrations were 2.6×10^{-5} M and 1.6×10^{-5} M, resp. The fluorescence depolarization was measured with a *JASCO FP-715* at 15° with [s-SPG] = 7.7×10^{-8} M.